Int J Clin Exp Pathol 2026;19(3):160-167
www.ijcep.com /ISSN:1936-2625/IJCEP0168458

Original Article

Exploration of the mechanism of hesperidin inhibition on the proliferation and metastasis of human breast cancer cells

Zhiyong Liu, Ran Chen

Breast Treatment Center, The First Affiliated Hospital of Gannan Medical University, Ganzhou 341000, Jiangxi, China

Received August 30, 2025; Accepted January 3, 2026; Epub March 15, 2026; Published March 30, 2026

Abstract: Objective: To investigate the mechanism of Hesperidin (Hsp) in inhibiting the proliferation and metastasis of breast cancer cell line MDA-MB-231. Methods: The effect of Hsp on cell survival rate was analyzed using the MTT assay. The anti-migration and anti-invasion abilities of Hesperidin were evaluated using the scratch test and Transwell migration assay. The activity of matrix metalloproteinases (MMP)-2/MMP-9 was analyzed using gelatin zymography. The expression of epithelial-mesenchymal transition (EMT)-related proteins (Vimentin, Snail, ZO-1) was detected by Western blot. Results: Low concentrations of Hsp (2-10 μmol/L) showed no significant cytotoxicity; 20-40 μmol/L significantly reduced survival rate ($P<0.01$). Scratch test results showed that Hsp inhibited wound healing in a concentration-dependent manner. Transwell migration assay showed that the number of migrating cells decreased with increasing Hsp concentration. Gelatin zymography results indicated that MMP-2/MMP-9 activity decreased with increasing Hsp concentration; Western Blotting results showed that Hsp downregulated the metastasis-related proteins Vimentin and Snail and upregulated the adhesion protein ZO-1. Conclusion: Our findings suggest that Hsp inhibits tumor cell invasion and metastasis by potentially reducing MMP-2/MMP-9 hydrolase activity, blocking extracellular matrix degradation, and reversing the EMT process (downregulating Vimentin/Snail and upregulating ZO-1). Hsp may represent a promising candidate for adjuvant therapy in breast cancer.

Keywords: Hesperidin, MDA-MB-231 cells, cell survival rate, cell proliferation, metastasis, epithelial-mesenchymal transition

Introduction

Breast cancer remains a leading cause of cancer-related mortality worldwide, with metastasis being a primary contributor to poor prognosis. Triple-negative breast cancer (TNBC), such as the MDA-MB-231 cell line, is particularly aggressive and lacks targeted therapeutic options, highlighting the need for novel treatment strategies. Hesperidin (Hsp), a typical flavonoid compound formed by the combination of hesperetin and rutin, belongs to the flavonoid derivatives and is widely distributed in citrus fruits [1]. This compound exhibits biological activities such as antioxidant, anti-inflammatory, and anti-tumor properties [2]. In vivo studies have revealed that hesperidin can reverse the biochemical and histopathological changes in blood caused by cisplatin and reduce the expression levels of Bax and Caspase3 proteins [3]. In vitro experiments further confirmed that hesperidin reverses neuronal apoptosis induced by a high glucose environment by inhibiting the expression of Caspase3 and Bax proteins [4]. Despite these broad activities, research on the mechanism of action of hesperidin on breast cancer, particularly its effects on invasion and metastasis, is relatively scarce. This study therefore aims to use the human triple-negative breast cancer cell line MDA-MB-231 as a model to explore the mechanism by which Hsp influences cancer cell survival, migration, and key molecular events in metastasis, including EMT.

https://doi.org/10.62347/BPFS2353

Materials and methods

Reagents and antibodies

Hesperidin (purity ≥98%, CAS 520-26-3) was purchased from Sigma-Aldrich (St. Louis, MO, USA). DMEM medium, fetal bovine serum (FBS), penicillin-streptomycin, and trypsin-EDTA were obtained from Gibco (Thermo Fisher Scientific, Waltham, MA, USA). The MTT assay kit and RIPA lysis buffer were purchased from Beyotime Biotechnology (Shanghai, China). Transwell chambers (8 μm pore size) were from Corning Inc. (Corning, NY, USA). Primary antibodies against Vimentin (ab92547, 1:1000), Snail (ab53519, 1:1000), ZO-1 (ab96587, 1:1000), and GAPDH (ab8245, 1:5000) were purchased from Abcam (Cambridge, UK). Horseradish peroxidase (HRP)-conjugated secondary antibodies were from Zhongshan Golden Bridge Biotechnology (Beijing, China). All other chemicals were of analytical grade.

Cell line

The human breast cancer cell line MDA-MB-231 was purchased from the Shanghai Cell Bank of the Chinese Academy of Sciences and was authenticated by short tandem repeat (STR) profiling. Cells were routinely tested and confirmed negative for mycoplasma contamination. Cells were cultured in DMEM medium containing 15% fetal bovine serum in a constant temperature incubator at 37°C with 5% CO_2. Cells were cultured and stored according to the supplier's instructions and used from the 5th to the 20th generation. All reagents used in this experiment were purchased from Fuzhou Maixin Biotechnology Co., Ltd., unless otherwise specified.

MTT assay

The concentration gradient of Hsp (2, 5, 10, 20, 40 μmol/L) was selected based on preliminary experiments and existing literature. The stock solution of Hsp was prepared in dimethyl sulfoxide (DMSO), and the final concentration of DMSO in all groups, including the control, did not exceed 0.1%.

Seed MDA-MB-231 cells into 96-well plates, with 5×10^3 cells per well, and six replicate wells were set up for each concentration. After the cells adhere to the plate, add different concentrations of Hsp, and incubate the plates in an incubator for 24 hours. After the incubation period, aspirate the culture medium from each well, add MTT solution (0.5 mg/100 μl) to each well, and then incubate the plates in the incubator for another 4 hours until a purple precipitate is visible. Discard the culture medium. Add 150 μl of DMSO to each well and shake for 10 minutes. Measure the absorbance of each well (including the blank control well) at a wavelength of 490 nanometers using a multi-mode microplate reader (EnSight™). The cell viability rate was calculated as follows: Viability (%) = (experimental group OD value - blank group OD value)/(control group OD value - blank group OD value) × 100%.

Scratch test

A wound healing experiment was conducted to assess the cell protrusion and migration abilities of tumor cells. MDA-MB-231 cells were seeded into 6-well plates with 1×10^6 cells per well and 2 ml of cell culture medium added. After the cells reached 100% confluence and formed a monolayer, scratches were made on the cell monolayer using a sterile 1 ml pipette tip, and debris was removed by rinsing with phosphate-buffered saline (PBS). The scraped cells were then washed away with PBS, and Hsp at different concentrations was prepared in DMEM/F12 containing 1% FBS to minimize cell proliferation. Incubation was carried out for another 24 hours. Cells that migrated to the wound area or protruded from the wound edge were observed and photographed under an inverted microscope. In each experiment, nine areas were randomly selected in each well, magnified at 100×, and the cells in each set of three wells were quantified. The experiment was repeated at least three times, with three replicates for each experiment.

Transwell assay

To assess cell migration, Transwell chambers with 8 μm pores were used. The lower chamber was filled with 650 μl of DMEM/F12 medium containing 10% fetal bovine serum (FBS) as a chemoattractant. The upper chamber was filled with 650 μl of serum-free DMEM/F12 medium. We added 1×10^4 cells resuspended in serum-free medium to each upper chamber and treated them with different concentrations of Hsp. After 24 hours of culture, non-migrated cells on the upper surface of the membrane were carefully removed with a cotton swab. The migrated cells on the lower surface were fixed with meth-

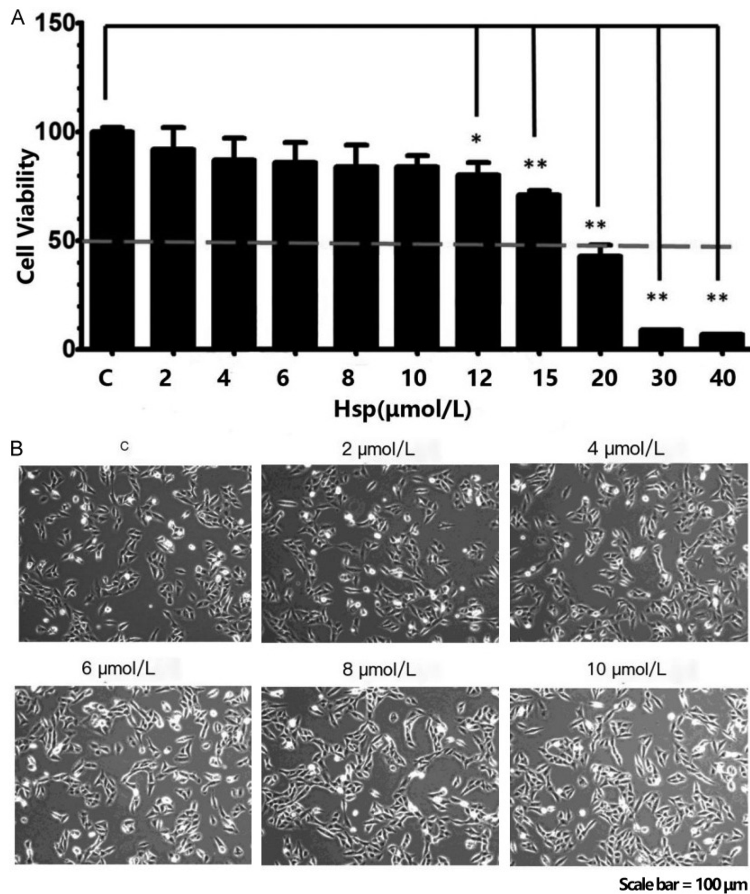

Figure 1. Effect of Hsp on the viability and morphology of MDA-MB-231 cells. A. MTT assay showing cell viability after 24 h treatment with various concentrations of Hsp. Data are presented as mean ± SD (n=6). *P<0.05, **P<0.01 vs. control (0 μmol/L). B. Representative phase-contrast images of cell morphology after Hsp treatment (Scale bar = 100 μm). c, Represents the control group.

anol for 15 minutes, then washed with PBS and stained with 0.1% crystal violet for 20 minutes. After air-drying, the cells that had invaded the lower surface were counted in at least 10 fields using a 200× microscope (Olympus). Each experiment was repeated at least three times.

Gelatin zymography test

The secretion of matrix metalloproteinase (MMP)-9 and MMP-2 was analyzed by gelatin zymography. First, cells were seeded in 24-well plates and cultured for one day until they adhered to the wall. After replacing with 10% of the culture medium, different concentrations of Hsp were added sequentially, and the cells were further cultured for 24 hours. After treatment, the culture medium was collected for subsequent gelatin zymography analysis. The samples were subjected to 0.1% sodium dodecyl sulfate-polyacrylamide gel electrophoresis (SDS-PAGE) using 10% gelatin. After electrophoretic separation in SDS buffer, the samples were washed with 2.5% Triton X-100, then placed in a buffer containing 150 mM NaCl, 50 mM Tris-HCl, and 10 mM $CaCl_2$, and incubated at 37°C for 20 hours. The gel was stained with 0.5% Coomassie blue solution, followed by destaining, and finally scanned and recorded.

Western blotting

Seed the cells into 10 cm culture dishes ($2×10^6$ cells per dish), and after they adhere to the wall, replace with medium of the desired drug concentration. Place the dishes in a 37°C, 5% CO_2 incubator and continue to incubate for 24 hours. Subsequently, scrape the cells from each group and collect them along with the medium into 15 ml centrifuge tubes. Centrifuge at 167.70 g for 5 minutes. Remove the supernatant and add 1 ml PBS to disperse the cells. Transfer to 1.5 ml centrifuge tubes and centrifuge at 6037.20 g for 5 minutes. Remove the supernatant, add an appropriate amount of RIPA lysis buffer containing 1% PMSF, and place on ice for 30 minutes. Lysates were then centrifuged at 12,000 g for 15 minutes at 4°C. After centrifugation, collect the supernatant, which contains total cellular protein. Protein concentration was determined using a BCA protein assay kit (Beyotime, China). Thirty micrograms of protein from each sample was separated by 10% SDS-PAGE and transferred to PVDF membranes (Millipore, USA). The membranes were blocked with 5% skim milk in TBST for 2 hours at room temperature and then incubated with primary antibodies against Vimentin (1:1000), Snail (1:1000), ZO-1 (1:1000), and GAPDH (1:5000) overnight at 4°C. The next day, after incubation with HRP-conjugated secondary

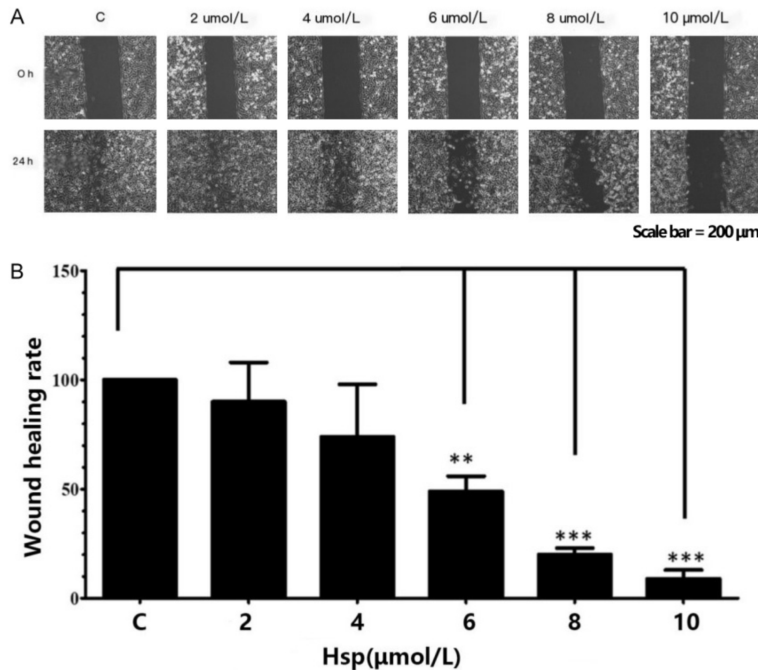

Figure 2. Hsp inhibits the migration of MDA-MB-231 cells in a scratch wound healing assay. A. Representative images of the scratch wound at 0 h and 24 h after treatment with different concentrations of Hsp (Scale bar = 200 μm). B. Quantitative analysis of the wound closure area. Data are presented as mean ± SD (n=3 independent experiments). ***P<0.001 vs. control.

antibodies for 1 hour at room temperature, protein bands were visualized using an enhanced chemiluminescence (ECL) detection kit (Tanon, China) and quantified using ImageJ software (NIH, USA). GAPDH was used as an internal loading control.

Statistical analysis

Experimental data are presented as mean ± standard deviation (SD) from at least three independent experiments. Statistical analysis was performed using GraphPad Prism 5 software (GraphPad Software, USA). Differences between multiple groups were analyzed by one-way analysis of variance (ANOVA) followed by Tukey's post-hoc test. Statistically significant differences are indicated by * (P<0.05), ** (P<0.01), and *** (P<0.001).

Results

The effect of Hsp on the survival of MDA-MB-231 cells

In **Figure 1A**, it is revealed through the MTT assay that Hsp does not exhibit significant cytotoxicity towards cells within the concentration range of 2-10 μmol/L. However, a significant decrease in survival rate can be observed at concentrations ranging from 20 to 40 μmol/L (P<0.01). Nevertheless, Hsp does not significantly alter the morphology of cancer cells at these concentrations (see **Figure 1B**).

The effect of Hsp on the migration and motility of MDA-MB-231 cells

The effect of Hsp on the migration and movement of MDA-MB-231 cells was observed using the scratch test and Transwell migration assay. The results showed that after treating MDA-MB-231 cells with Hsp for 24 hours, there was a significant difference in migration between the Hsp-treated cells and the control group (**Figure 2A**). Quantifying the migration area using Image J software, it was observed that after treating MDA-MB-231 cells with Hsp for 24 hours, cell migration was significantly inhibited as the Hsp concentration increased (**Figure 2B**). Continuing to observe the effect of Hsp on the migration of MDA-MB-231 cells using Transwell, the number of cells that migrated to the lower chamber was observed after treating with Hsp for 24 hours using crystal violet staining. As shown in **Figure 3A**, it was observed that as the drug concentration increased, the number of MDA-MB-231 cells that migrated to the lower chamber showed a decreasing trend. Quantitative analysis (**Figure 3B**) showed a significant reduction in migrated cells compared to the control.

The effect of Hsp on the activity of matrix metalloproteinases MMP-2 and MMP-9 in MDA-MB-231 cells

The expression levels of matrix metalloproteinases (MMP-2 and MMP-9) after Hsp treatment were studied using gelatin zymography. The results indicated that as the drug concentration increased, the activity of matrix metalloproteinases (MMP-2 and MMP-9) associated

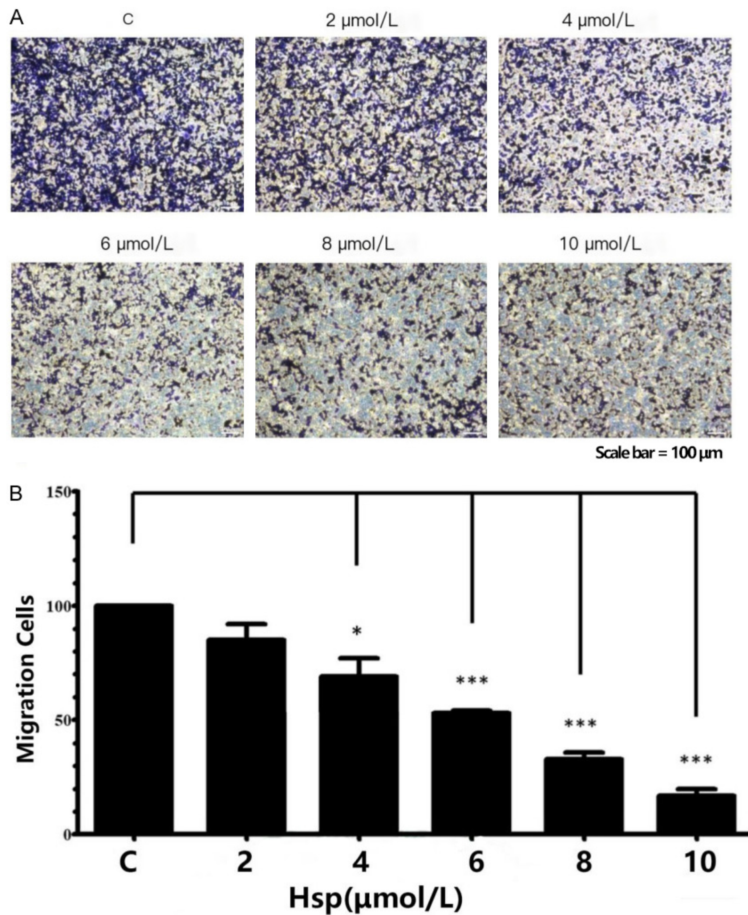

Figure 3. Hsp inhibits the migration of MDA-MB-231 cells in a Transwell assay. A. Representative images of crystal violet-stained migrated cells on the lower surface of the membrane (Scale bar =100 μm). B. Quantitative analysis of the number of migrated cells per field. Data are presented as mean ± SD (n=3 independent experiments). **P<0.01, ***P<0.001 vs. control.

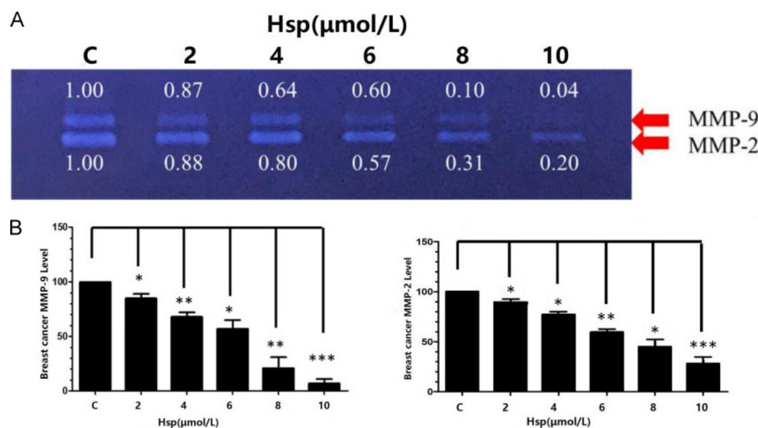

Figure 4. Hsp reduces the activity of MMP-2 and MMP-9 in MDA-MB-231 cells. A. Gelatin zymography gel showing MMP-2 and MMP-9 activity. B. Densitometric analysis of MMP-2 and MMP-9 band intensities. Data are presented as mean ± SD (n=3). *P<0.05, **P<0.01 vs. control.

with cell metastasis decreased (**Figure 4A**). Densitometric analysis confirmed a concentration-dependent inhibition of both MMP-2 and MMP-9 activities (**Figure 4B**).

The effect of Hsp on the expression levels of proteins related to epithelial-mesenchymal transition in MDA-MB-231 cells

As shown in **Figure 5A**, in MDA-MB-231 cells treated with Hsp, the protein expression levels of vimentin and snail decreased, while the expression level of ZO-1 increased. Densitometric analysis normalized to GAPDH (**Figure 5B**) revealed that Hsp treatment significantly down-regulated Vimentin and Snail expression (P<0.01), and upregulated ZO-1 expression (P<0.01) compared to the control. This indicates that as the drug concentration increases, the expression levels of proteins related to cell metastasis decrease, while those related to adhesion increase. This process, in turn, blocks a key step in epithelial-mesenchymal transition (EMT).

Discussion

In this study, we demonstrated that Hesperidin (Hsp) effectively inhibits the migration and invasion of the highly aggressive MDA-MB-231 breast cancer cell line. Our data suggests that the underlying mechanism involves the suppression of MMP-2/MMP-9 activity and the reversal of key EMT markers.

The MTT assay established a non-cytotoxic concentration range (2-10 μmol/L) for subsequent functional experiments, while higher concentrations

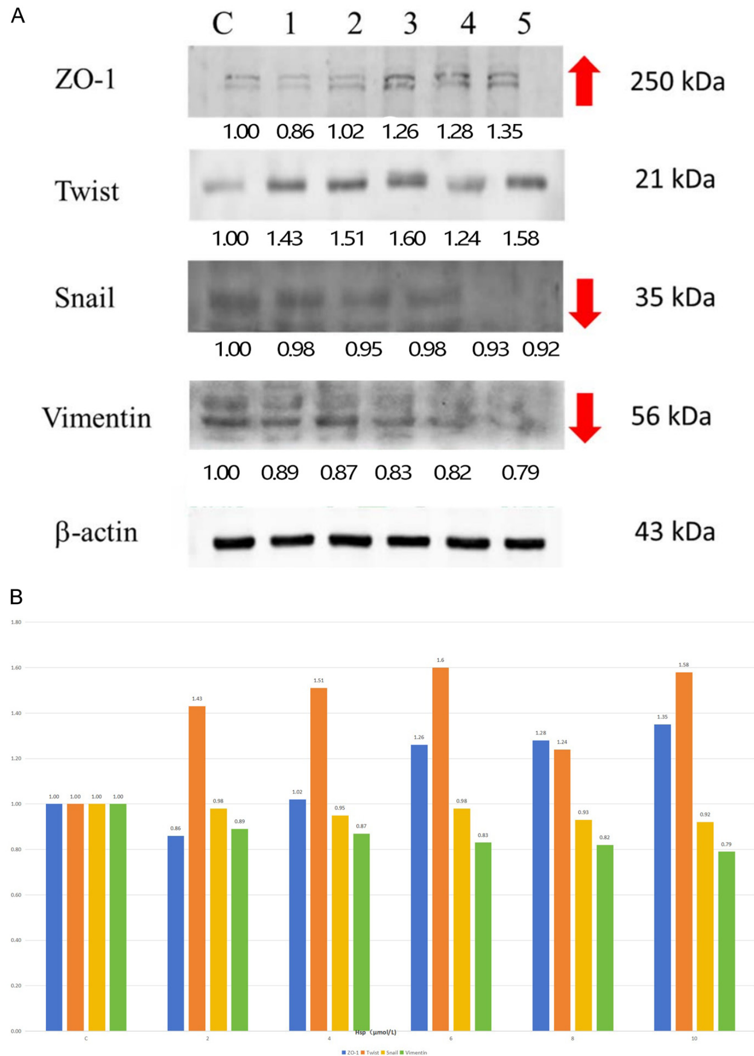

Figure 5. Hsp reverses epithelial-mesenchymal transition (EMT) in MDA-MB-231 cells. Western blot analysis of Vimentin, Snail, and ZO-1 protein expression. GAPDH was used as a loading control. Densitometric quantification of protein levels normalized to GAPDH. Data are presented as mean ± SD (n=3). *P<0.05, **P<0.01 vs. control.

(20-40 μmol/L) significantly reduced cell viability. This biphasic effect is consistent with the concept of a therapeutic window for natural compounds [5]. Our findings align with a previous report showing Hsp's cytotoxic effects on other cancer cell types [6-9], but we provide new evidence for its anti-migratory effects in TNBC.

Cell migration is a critical step in cancer metastasis. Using scratch wound healing and Transwell migration assays, we found that Hsp significantly impeded the migratory capacity of MDA-MB-231 cells in a concentration-dependent manner, even at lower concentrations that were not cytotoxic. This indicates that the anti-migratory effect of Hsp is, at least partially, independent of its effect on cell proliferation or survival. Similar anti-migratory effects of Hsp have been observed in other cancers, such as colon and liver cancer [10, 11], but data on breast cancer, particularly TNBC, remains limited.

Metastasizing cells degrade the extracellular matrix (ECM) primarily through the action of MMPs. Our gelatin zymography results clearly showed that Hsp treatment led to a significant reduction in the activities of MMP-2 and MMP-9. This finding is crucial, as MMP-2 and MMP-9 are strongly implicated in breast cancer progression and poor prognosis [12-15]. The inhibition of these enzymes by Hsp likely contributes to the observed reduction in cell migration by preventing ECM remodeling.

The EMT process is a hallmark of cancer metastasis, characterized by loss of epithelial markers (e.g., E-cadherin, ZO-1) and gain of mesenchymal markers (e.g., Vimentin, Snail) [16-18]. In our study, Western blot analysis revealed that Hsp treatment downregulated the expression of the mesenchymal markers Vimentin and Snail, while concurrently upregulating the tight junction protein ZO-1, an epithelial marker. The downregulation of Snail, a key transcriptional repressor of E-cadherin, is particularly significant. However, in some cancer cells with high metastatic ability, E-cadherin may not necessarily be expressed, so it is possible to detect the protein ZO-1 related to adhesion factors [19]. The upregulation of ZO-1 provides strong evidence for a reversal of the EMT phenotype. Our results are supported by a recent study showing that Hsp could modulate EMT markers in a different biological context [20]. The collective downregulation of MMP activity and reversal of EMT mark-

ers by Hsp suggests a multi-faceted mechanism against metastasis.

Conclusion

In conclusion, our study provides evidence that Hesperidin inhibits the migration and invasion of MDA-MB-231 breast cancer cells. The anti-metastatic effects are associated with the downregulation of MMP-2/MMP-9 activity and the reversal of the EMT process, characterized by decreased Vimentin/Snail and increased ZO-1 expression. These findings suggest that Hesperidin holds promise as a potential adjuvant therapeutic agent for breast cancer, warranting further investigation in vivo to validate its efficacy and elucidate the precise upstream signaling pathways involved.

Acknowledgements

We express our gratitude to the First Affiliated Hospital of Gannan Medical University for support.

Disclosure of conflict of interest

None.

Address correspondence to: Dr. Zhiyong Liu, Breast Diagnosis and Treatment Center, Huangjin Branch, The First Affiliated Hospital of Gannan Medical University, No. 128 Jinling Road, Huangjin Technology Development Zone, Ganzhou 341000, Jiangxi, China. Tel: +86-15807073854; E-mail: barton123321@163.com

References

[1] Yang Y, Yang XF, Huang PS, Leng J, Yang F and LI YJ. Inhibitory effect of hesperetin on estrogen and progesterone-induced breast hyperplasia in female rats. Chin J Clin Pharmacol 2024; 40: 77-81.

[2] Wang QR, Liu RX, He X, Zhang T and Zhao XH. Progress on pharmacological effects and improving solubility technologies of hesperidi. Prog Vet Med 2025; 46: 91-96.

[3] Aboraya DM, El Baz A, Risha EF and Abdelhamid FM. Hesperidin ameliorates cisplatin induced hepatotoxicity and attenuates oxidative damage, cell apoptosis, and inflammation in rats. Saudi J Biol Sci 2022; 29: 3157-3166.

[4] Lim C, Zhen AX, Ok S, Fernando PDSM, Herath HMUL, Piao MJ, Kang KA and Hyun JW. Hesperidin protects SH-SY5Y neuronal cells against high glucose-induced apoptosis via regulation of MAPK signaling. Antioxidants (Basel) 2022; 11: 1707-1719.

[5] Shi J, Li J, Xu Z, Chen L, Luo R, Zhang C, Gao F, Zhang J and Fu C. Celastrol: a review of useful strategies overcoming its limitation in anticancer application. Front Pharmacol 2020; 11: 558741-558765.

[6] Ramezanimoladehi M, Sheikhzadeh S and Delirezh N. Synergistic apoptotic effects of berberine and hesperidin co-encapsulated in PLGA nanoparticles on lymph node carcinoma of prostate cell line. Biomed Pharmacother 2025; 191: 118455-118471.

[7] Özdemir İ, Afşin Y, Tuncer MC and Öztürk Ş. Combined hesperidin and doxorubicin treatment induces apoptosis and modulates inflammatory cytokines in hela cervical cancer cells. Int J Mol Sci 2025; 26: 8753-8775.

[8] Afşin Y, Özdemir İ, Toprak V, Tuncer MC and Öztürk Ş. Combined hesperidin and gemcitabine therapy modulates apoptosis and angiogenesis pathways in ISHIKAWA human endometrial adenocarcinoma cells. Medicina (Kaunas) 2025; 61: 1599-1615.

[9] Karabat MU, Tuncer MC and Özdemir İ. In vitro evaluation of cytotoxic and pro-apoptotic effects of hesperidin alone and in combination with cisplatin on human malignant melanoma cell line (A431). Pharmaceuticals (Basel) 2025; 18: 854-869.

[10] Sun KX, Tan WS, Wang HY, Gao JM, Wang SY, Xie ML and Deng WL. Hesperidin suppressed colorectal cancer through inhibition of glycolysis. Chin J Integr Med 2025; 31: 529-540.

[11] Samodien S, de Kock M, Joubert E, de Beer D, Kriel J, Gelderblom WCA and Lilly M. Autophagy-induced cell death by aqueous and polyphenol-enriched extracts of honeybush (*Cyclopia* spp.) in liver and colon cancer cells. Food Sci Nutr 2024; 12: 5647-5662.

[12] Ramadan DR, Osman HA, Madhy SA, Teleb M, Darwish AI, Abu-Serie MM, Haiba NS, Khattab SN and Khalil HH. A tailored 4G *s*-triazine-based dendrimer vehicle for quercetin endowed with MMP-2/9 inhibition and VEGF downregulation for targeting breast cancer progression and liver metastasis. RSC Adv 2025; 15: 10426-10441.

[13] Latronico T, Petraglia T, Sileo C, Bilancia D, Rossano R and Liuzzi GM. Inhibition of MMP-2 and MMP-9 by dietary antioxidants in THP-1 macrophages and sera from patients with breast cancer. Molecules 2024; 29: 1718-1742.

[14] Jayaprakash B, Suresh AR, Thiruvengadam R, Alharbi NS, Kadaikunnan S, Sankaran S, Thiruvengadam M, Senthil R and Venkidasamy B. Evaluation of oyster mushroom (*Pleurotus ostreatus*)-derived anthraquinone on the in-

duction of apoptosis and suppression of MMP-2 and MMP-9 expression in breast cancer cells. Int J Med Sci 2024; 21: 1016-1026.
[15] Rao Q, Yu H, Li R, He B, Wang Y, Guo X, Zhao G and Wu F. Dihydroartemisinin inhibits angiogenesis in breast cancer via regulating VEGF and MMP-2/-9. Fundam Clin Pharmacol 2024; 38: 113-125.
[16] Lin WD, Chen YC, Lin FC, Pan JK, Chen MH, Chen HL, Chung WP, Cheng HC, Hsiao M, Yang CN and Lu PJ. Loss of estrogen receptor alpha promotes distant metastasis through epithelial-mesenchymal transition in luminal-type breast cancer. Biochim Biophys Acta Mol Basis Dis 2026; 1872: 168055-168067.
[17] Lee YJ, Park SH, Oh B, Yoon SJ, Lee SJ, Choi S, Kim MJ, Kim J, Cho YL, Kim W, Ku BJ and Park YJ. Particulate matter-induced lung cancer metastasis is inhibited by ginsenoside Rg3. J Environ Sci (China) 2025; 158: 60-71.
[18] Chang TM, Fang WY, Hsu HP, Chu PY, Jiang SS, Huang KW, Hung WC, Lin HY and Tsai HJ. *PCK2* promotes invasion and epithelial-to-mesenchymal transition in triple-negative breast cancer by promoting TGF-β/SMAD3 signaling through inhibiting TRIM67-mediated SMAD3 ubiquitination. Cancer Biol Ther 2025; 26: 2478670-2478682.
[19] Huang X, Luo W, Liu W, Liu X and Chen W. Progerin regulates actin cytoskeletal remodeling and inhibits EMT and metastasis in triple-negative breast cancer cells. Int J Oncol 2025; 67: 92-104.
[20] Liang Z, Zhang Y, Xu Y, Zhang X and Wang Y. Hesperidin inhibits tobacco smoke-induced pulmonary cell proliferation and EMT in mouse lung tissues via the p38 signaling pathway. Oncol Lett 2022; 25: 30-37.